Influence of the source geometry on the helium $He^M(2^3S)$ metastable atoms production in a He/O_2 plasma jet impacting on liquid surface

L. Invernizzi[1], N. Sadeghi[2,3], F. P. Sainct[1] and Ph. Guillot[1]

[1]Laboratoire Diagnostics des Plasmas Hors Equilibre, DPHE, Université de Toulouse, INU Champollion, Albi, France
[2]LIPhy UMR5588, Université Joseph Fourier - CNRS, Grenoble, France
[3]LTM UMR5129, Université Joseph Fourier - CNRS, Grenoble, France

Abstract: Space-time evolutions of both the densities and lifetimes of helium $He^M(2^3S)$ metastable atoms in a He/O_2 plasma jet in interaction with a liquid are measured by tunable diode laser absorption spectroscopy. The study of the source geometry, asymmetric or symmetric, shows that the asymmetric source is preferable to maximize the density of He^M in the plasma jet whereas their lifetimes are slightly shorter in the symmetric source.

Keywords: He^M(23S) , TDLAS, plasma source geometry, plasma-liquid interaction.

1. Introduction

Since the last two decades, there is a growing interest in plasma jet development and characterization due to the large number of possible applications. One of them is the decontamination of liquids, as the corresponding plasma has a high oxidative capacity. Plasma jet in contact with liquid generates reactive oxygen and nitrogen species (RONS), electric field, charged species, UV and VUV radiation, that may trigger the oxidation processes for the contaminant removal in solution [1–3]. The creation of RONS is one of the main mechanism in the gas phase via the energy transfer between the air molecules and the rare gas atoms feeding the discharge.

Metastable helium atoms (He^M) store an energy of 19.8 eV and can release it in three-body collision with two He atoms or in collision with others gases present as impurity. N_2 and O_2 are good quencher of these metastable states, leading to the creation of RONS. The density of He^M in the plasma jet depends on the voltage applied, the purity of the gas and the mixing with air.

The non-intrusive method used to quantify the He^M density is based on tunable diode laser absorption spectroscopy (TDLAS) [4–6]. The laser goes through the plasma jet and is attenuated by the targeted species. The absolute density and the lifetime of He^M along the laser line of sight temporally and spatially resolved is then deduced.

In this work, the focus is made on the influence of the source geometry on the densities and the lifetime of He^M when the plasma jet is in interaction with a liquid target.

2. Experimental setup

The experimental setup consists of an atmospheric pressure plasma jet (APPJ) generated in an asymmetric or in a symmetric source in contact with a liquid target. Fig. 1 (a) and (b) represents a plasma jet generated by the asymmetric and symmetric source respectively impacting on liquid surface. The high-voltage electrode is placed around a 3.7 mm inner diameter tube, and the grounded electrode is placed around a 36 mm inner diameter tube. The symmetric source (Fig. 1 (b)) consists of a tube of a 3.7 mm inner diameter tube. The feeding gas is helium with a small admixture of oxygen (0.2 %) at 0.5 L.min^{-1} flow rate.

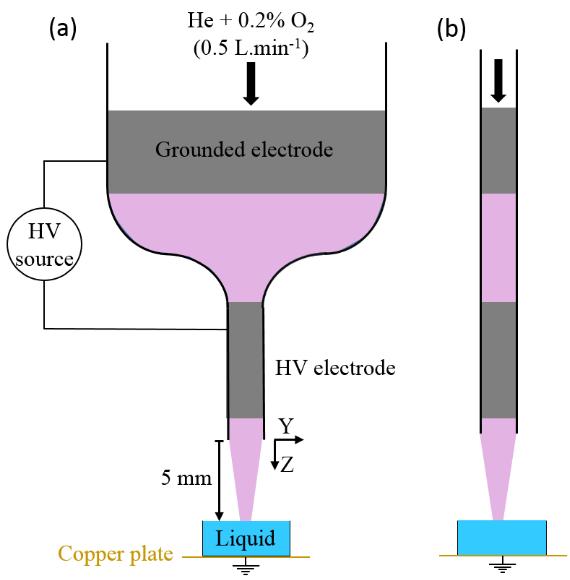

Fig. 1. Schematic diagram of the liquid treatment by the plasma jet generated in the asymmetric source (a) and in the symmetric source (b).

A glass container completely filled with 22 mL ultra-pure water (MilliQ, Direct Q3 Millipore) was used as a target for the plasma treatment. The distance between the edge of the source and the liquid target was set to 5 mm. The gap between the source and the liquid was small enough for the plasma to touch the liquid.

The high voltage power supply (NanoGen1, RLC SARL) connected to the electrode provides a 6 kV positive voltage pulse with 8 ns pulse rise time, 2.5 µs duration (5% duty cycle) 20 kHz repetition rate. The typical voltage and total current signals are represented in Fig. 2.

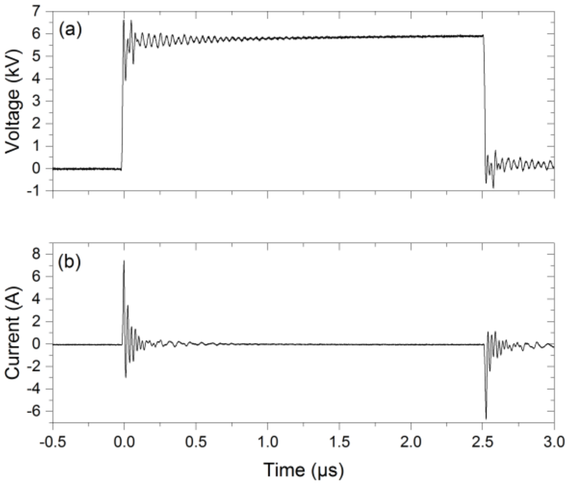

Fig. 2. Typical voltage (a) and current (b) waveforms (6 kV, 2.5 µs pulse duration).

The voltage measurements were performed with a voltage probe, model P6015A, Tektronix. The current was measured by a current probe (model 6585, Pearson). In order to determine the energy deposited in the discharge, the discharge current is required. The total current, due to both capacitive and discharge contributions, as shown in Fig. 2 (b), was measured when the plasma is present. Then the capacitive current was measured when the plasma is switched off. For this purpose the feeding gas has been replaced by air, in which no plasma is generated when a 6 kV is applied to the HV electrode. After subtraction of the capacitive current from the total current, the discharge current is obtained. The energy deposited in the discharge is then calculated using the time integration of the product of the discharge current and the voltage.

Tunable diode laser absorption spectroscopy was performed with a distributed feedback laser diode (Toptica, DL 100) emitting around 1083 nm. The spatio-temporal distribution of He^M in the plasma outside the dielectric tube is measured using the ($2^3P_J \leftarrow 2^3S_1$) helium transition where J = 0, 1 or 2. Vertical lines in Fig. 3 show the relative positions and intensities of the three components of the line. The normalized profile of the whole line at atmospheric pressure for a gas temperature of 440 K and a He^M density of 10^{13} cm^{-3} is also shown. At atmospheric pressure, the pressure broadening is relatively large and the lines corresponding to J = 1 and J = 2 are combined.

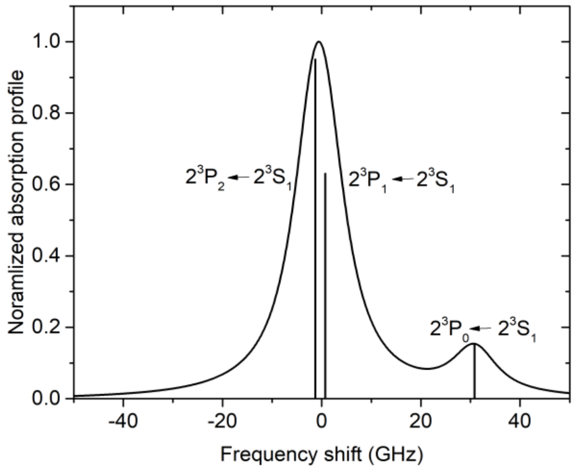

Fig. 3. Normalized absorptions profile (line) and theoretical positions and intensities (vertical lines) of the $2^3P_J \leftarrow 2^3S_1$ transitions for He^M density of 10^{13} cm^{-3}.

The method used to measure the He^M densities consists in setting the laser wavelength at the center of the two transitions $2^3P_{1,2} \leftarrow 2^3S_1$. The intensity of the transmitted beam is measured with an InGaAs photodiode (New Focus, model 1811) and is converted into the absorbance using the Beer-Lambert's law. The absolute He^M density along the laser line of sight is then deduced at a given axial position. The exponential decay observed right after the maximal density provides the lifetime of He^M.

The TDLAS experimental setup is shown in Fig. 4. A set of lenses provide a laser spot of around 100 µm diameter in the jet positions (spatial resolution). The response time of the InGaAs detector, which collects the laser beam behind the plasma jet is 3 ns. A Fabry-Pérot and a low pressure helium lamp are used to set the laser at the wavelength corresponding to the lines J =1 and 2.

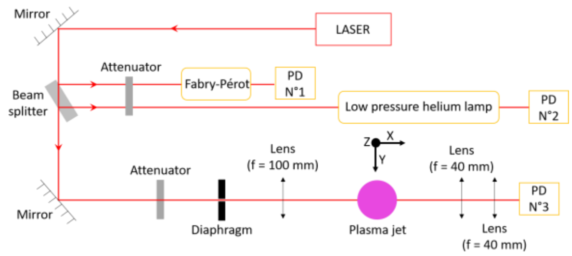

Fig. 4. Experimental laser setup for the measurement of He^M density.

The profiles represented in this work are integrated along the laser line of sight (X direction, see Fig. 4). In some cases, the horizontal axis is called "Y position" because radial position would indicate that Abel's inversion has been performed, which is not the case.

3. Results and discussion

Fig. 5 represents the time variation of the mean He^M density over 3 mm, when the laser probes the plasma at the outlet of the source (Z = 0 mm) and at the plasma jet axis (Y = 0 mm). (a) for the asymmetric and (b) for the symmetric configurations.

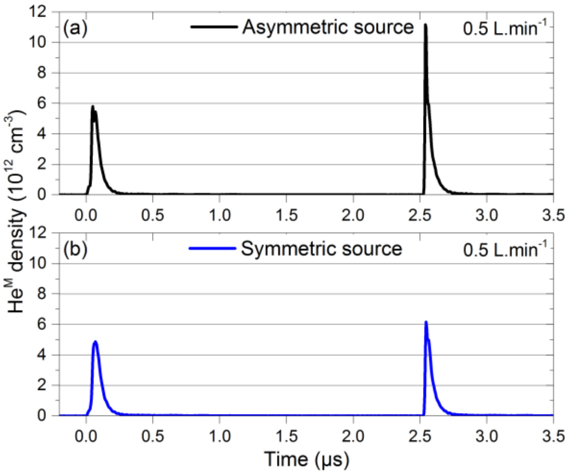

Fig. 5. Temporal evolution of He^M density at the outlet edge of the source and at the plasma axis for the asymmetric (a) and the symmetric (b) sources.

As the voltage pulse begins at t = 0 µs and stops at t = 2.5 µs, two He^M peaks are produced. The two creation times of He^M are short (one hundred of nanosecond), followed by an exponential decay due to the collisions of the He^M with the 0.2% O_2 present in the feed gas. The shape of the densities are very similar for both sources. During the falling front peaks, the He^M production with the asymmetric source has doubled compare to the symmetric one. This difference may be explained by the higher energy deposited in the discharge with the asymmetric source than the symmetric one, due to the smaller area of the mass electrode in the last case. However, the source geometry seems to have much less influence on these densities during the rising front: the He^M production processes are different according to the studied pulse fronts. It is also possible that the larger He^M densities in the falling edge and in the asymmetric configuration could be linked to a lower O_2 density in the outlet of the tube. In fact, O_2, which is the main quencher of He^M, should be more dissociated after the falling edge when the gas was subject to two discharge pulses (one in the rising edge followed immediately by another in the falling edge). Similarly, the residence time of the gas inside the discharge volume is larger for the asymmetric source and consequently the gas is subject to many discharge pulses, leading to a lower O_2 amount.

Fig. 6 focuses on the Y position (see Fig. 1 and Fig. 4) evolution of the maximum He^M densities (peaks) for each front and each source at the outlet of the considered source.

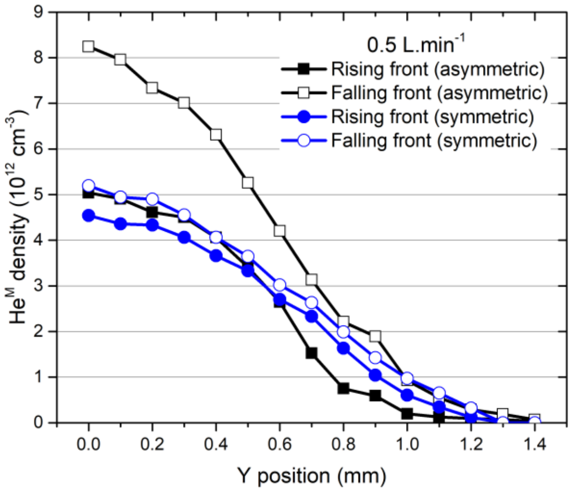

Fig. 6. Y position evolution of He^M density at the outlet edge of the source for the two fronts in both sources.

In all situations, the He^M density decreases with the increase of the Y position (i.e. the laser is moved to the plasma edge), regardless of the front and the source geometry. This may be explain by the electric field intensity decrease along the Y position. Therefore, He^M production by electronic collisions are less frequent at the outlet edge of the plasma.

To better understand the He^M production mechanisms with the two sources during the fronts, Fig. 7 presents the He^M lifetimes evolutions as a function of the Y position.

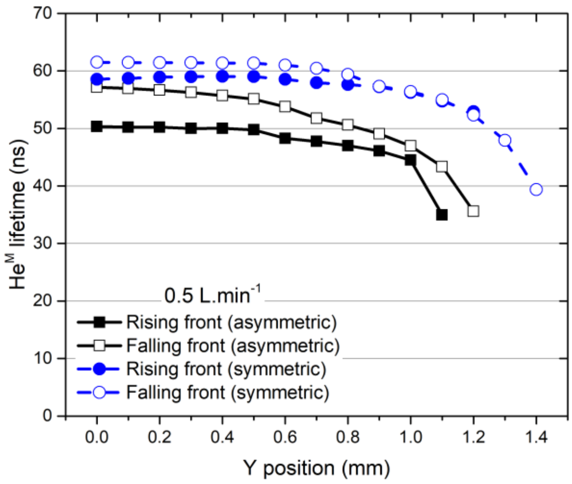

Fig. 7. Y position evolution of He^M lifetime at the outlet edge of the source for the two fronts in both sources.

The He^M lifetimes measured with the symmetric source are comparable for the two fronts. Conversely, there is a difference between the two fronts in the asymmetric source. The decay of He^M density is about ten nanoseconds faster in the rising front than in the falling one. Lower lifetime values indicate more He^M quenching processes.

The flow influence has also been investigated to underline the He^M density evolution as shown in Fig. 8 for 0.5 and 2 $L.min^{-1}$.

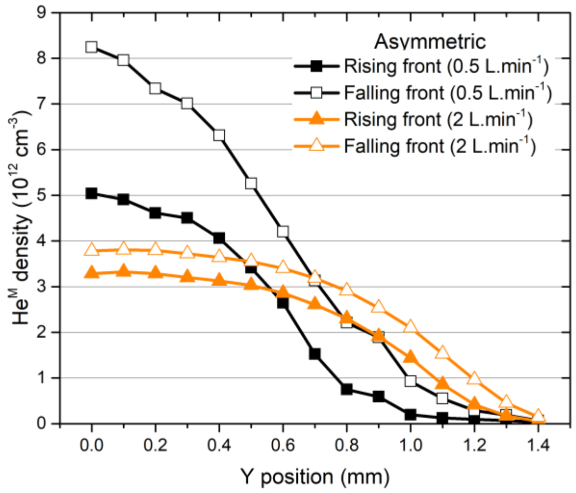

Fig. 8. Y position evolution of He^M density at the outlet edge of the asymmetric source for the two fronts and two flows.

The total absorption length is higher in the case of the largest flow rate. Moreover, the He^M densities measured with the highest flow show a plateau at the center during few hundreds of micrometers. This particular shape is generally associated to a pure helium plasma jet. In this case a He^M density annular shape appears at the outlet edge of the source, due to the excitation profile with a ring shape too.

4. Conclusion

The characterization of atmospheric pressure plasma jets is a challenge as the physics and chemistry associated are complex. Helium/oxygen plasma jet contains metastable helium atoms that govern the reactivity of the plasma. The energy transfer between the plasma and the surrounding air is partly due to He^M and the high energy they store (19.8 eV). The admixture of O_2 from the feed gas and of N_2 and O_2 from the air, enable the plasma jet to produce reactive oxygen and nitrogen species, capable of reacting with many types of targets depending on the application.

Using the tunable diode laser absorption spectroscopy technique, both densities and lifetimes of He^M have been measured to highlight differences of plasma generated in two different sources. One of them has an asymmetric geometry while the second has a symmetric geometry. The difference comes from the area of the mass electrode which is bigger in the case of the asymmetric source. As a result, the plasma generated in the asymmetric source produces more He^M during the falling front of the pulse. The radial variation of the He^M density may be explained by the electric field intensity which is lower at the edge of the plasma. A lower electron temperature at the plasma edge should produce less He^M atoms. The lifetime of He^M is slightly longer in the center of the discharge (50-60 ns) than at the edge of the plasma (40-50 ns). The increase of the gas flow causes a ring shape of He^M density at the outlet edge of the source as the excitation profile seems to have a ring shape with the highest flow rate.

5. Acknowledgments

This work was supported by Occitanie region. The “Réseau Plasma Froids” of CNRS/MRCT (France) is acknowledged for providing the DFB diode laser as well as the IPMC for the travel support for Nader Sadeghi.

6. References

[1] Xu H, Liu D, Wang W, Liu Z, Guo L, Rong M and Kong M G 2018 Investigation on the RONS and bactericidal effects induced by He + O2 cold plasma jets: In open air and in an airtight chamber *Physics of Plasmas* **25** 113506

[2] Schneider S, Lackmann J-W, Ellerweg D, Denis B, Narberhaus F, Bandow J E and Benedikt J 2012 The Role of VUV Radiation in the Inactivation of Bacteria with an Atmospheric Pressure Plasma Jet *Plasma Processes and Polymers* **9** 561–8

[3] Leduc M, Guay D, Leask R L and Coulombe S 2009 Cell permeabilization using a non-thermal plasma *New J. Phys.* **11** 115021

[4] Darny T, Pouvesle J-M, Fontane J, Joly L, Dozias S and Robert E 2017 Plasma action on helium flow in cold atmospheric pressure plasma jet experiments *Plasma Sources Sci. Technol.* **26** 105001

[5] Lu X, Naidis G V, Laroussi M, Reuter S, Graves D B and Ostrikov K 2016 Reactive species in non-equilibrium atmospheric-pressure plasmas: Generation, transport, and biological effects *Physics Reports* **630** 1–84

[6] Urabe K, Morita T, Tachibana K and Ganguly B N 2010 Investigation of discharge mechanisms in helium plasma jet at atmospheric pressure by laser spectroscopic measurements *J. Phys. D: Appl. Phys.* **43** 095201